Effect of s-d hybridization on interatomic pair potentials of the 3d liquid transition metals

1993 J. Phys.: Condens. Matter 5 1901

(http://iopscience.iop.org/0953-8984/5/13/008)

J. Phys.: Condens. Matter 5 (1993) 1901–1918. Printed in the UK

Effect of s–d hybridization on interatomic pair potentials of the 3d liquid transition metals

L Do Phuong, A Pasturel and D Nguyen Manh†

Laboratoire de Thermodynamique et de Physico-Chimie Métallurgiques, ENSEEG, BP 75, 38402 St-Martin-d'Hères Cédex, France

Received 16 October 1992, in final form 22 December 1992

Abstract. We have derived interatomic pair potentials for liquid transition metals using the tight-binding cluster Bethe lattice method (CBLM) in which the important role of s electrons (changing the number d electrons, screening d charge transfer and band mixing effect via s–d hybridization) can be treated self-consistently. Coupled with molecular dynamics simulations, we have calculated the static structure factors $S(q)$ of the 3d liquid transition metals, which are in good agreement with the experimental ones. The results for the electronic density of states of these metals as well as their cohesive energy are also presented. We have also discussed our results in the light of those obtained in the Wills–Harrison and Pettifor models.

1. Introduction

Very recently, there have been a few advanced studies of interatomic interactions for transition metals. Mosts of these works are based on a study of Wills and Harrison (WH) [1], who used a separate treatment for sp and d states, leading to an effective pair potential that takes into account the role of s electrons in changing the number of d electrons. The WH pair potential has been used to determine the thermodynamic properties of liquid transition metals by applying the Gibbs–Bogoliubov variational scheme with hard-sphere [2], hard-sphere Yukawa [3] and charged hard-sphere [4] fluid as a reference system. However, as has been analysed and tested by Regnaut [5], the very deep potential well predicted in the WH model for its first minimum and its position lead to many difficulties in describing the structure of transition metals with half-filled and less than half-filled d bands. The deficiencies of the WH model can be explained by the crudeness of the treatment of s–d hybridization as well as the neglect of multi-ion potentials [6].

These difficulties can be overcome in an alternative approach developed by Pettifor in the tight-binding (TB) bond model derived from first principles within density-functional theory [7, 8]. In this model, an angular-dependent many-body potential expression for the bond order, which gives the direct dependence of the bond strength on the local atomic environment, can be obtained. The explicit analytic form of these many-body potentials has the necessary ingredients for an adequate description, but there are difficulties in practice when it comes to incorporating the charge-transfer contribution between different orbitals in a self-consistent manner.

† Permanent address: Department of Physics, Polytechnic University of Hanoi, Vietnam

0953-8984/93/131901+18$07.50

Whereas there is strong evidence that the contributions of multi-ion terms are necessary in the study of solid transition metals, it is believed that progress in the understanding of their liquid-state properties may only come about by using effective pair potentials [4] that take accurate account of the important s–d hybridization and charge-transfer contributions.

The last remark has encouraged us to develop a new simple effective pair interaction for disordered (liquid, in particular) transition metals, which possesses the correct attributes of the s electrons in a self-consistent description of their liquid structures. Our formalism is based on the tight-binding scalar cluster Bethe lattice method (SCBLM) [9], which is expected to be valid in disordered systems. This method has enabled us to study successfully the sp–d hybridization in some transition alloys and to determine chemical short-range order from a self-consistent calculation of charge transfer [10, 11]. Since the fourth moment of the local density of states, μ_4, which characterizes the band-mixing effect, can be reproduced accurately from the SCBLM [12], we hope that the TB bond contribution derived from this model will be improved in comparison with an embedding potential [13, 14] through the second moment μ_2 approximation. It is interesting to note that Hausleitner and Hafner have recently calculated the bond order to interatomic forces in disordered transition-metal alloys using a Bethe lattice reference, but taking into account only the d-electron contribution, the s–d hybridization matrix element in their model Hamiltonian being completely neglected [15]. However, it is known that s–d hybridization plays a non-negligible role in transition-metal cohesive properties [16] and produces changes in predictions for phase stability.

In the next section we present the derivation of the interatomic interactions in the SCBLM scheme and illustrate in detail the attractive and repulsive pairwise contributions to the total energy in the case where the distance dependence of the hopping integrals is assumed to follow the power law r^{-q}. In section 3 we couple these interatomic interactions with a molecular dynamics simulation to study the liquid structures of the 3d transition metals. More particularly, we show that our interactions yield reasonable agreement between calculated static structure factors $S(q)$ and the experimental ones. In section 4, studies of the electronic structure and of the cohesive energy of these metals are presented to stress the importance of the s–d hybridization effect. In section 5 we complete our results with a discussion and the possibility to extend this model in the case of transition-metal alloys. Finally, we make explicit the relation between the power-law parametrization of the pair potential and the binding-energy universality in the appendix.

2. Theoretical approach to interactomic forces

2.1. Total energy

The total energy derived from first principles within the density-functional theory can be written in the form [7]

$$U = U_{\text{rep}} + U_{\text{bond}} + U_{\text{prom}} \tag{1}$$

where U_{rep} is a semi-empirical pairwise repulsive contribution, namely

$$U_{\text{rep}} = \tfrac{1}{2} \sum_{ij, i \neq j} \Phi_{\text{rep}}(R_{ij}) \tag{2}$$

and U_{bond} is the covalent bond energy that results from computing the local electronic density of states (LDOS) $n_{i\alpha}(E)$ associated with orbital α on site i within the two-centre orthogonal tight-binding approximation. Then we obtain

$$U_{\text{bond}} = \sum_{i\alpha} \int^{E_F} (E - E_{i\alpha}) n_{i\alpha}(E)\, dE \tag{3}$$

where $E_{i\alpha}$ is the effective atomic energy level of orbital α at site i and E_F is the Fermi energy. In the derivation of equation (1) from first principles [7], the pairwise nature of the repulsive term follows directly from the Harris–Foulkes approximation to density-functional theory [17], whereas the Hückel-type two-centre orthogonal form of the matrix elements may be justified from either chemical pseudopotential [18] or muffin-type orbital theory [19].

The third contribution in equation (1) is the promotion energy, which takes into account the change in occupancy of an energy level of orbital α on going from the reference free-atom state to a given bonding situation. In general, this contribution depends also on the charge transfer between orbitals in each considered state. Assuming that the crystal-energy-field terms produce identical shifts for the s and d atomic energies on a given site in the case of transition-metal systems, the promotion energy can be defined by [20]

$$U_{\text{prom}} = (E_d^0 - E_s^0)\Delta N \tag{4}$$

where E_s^0 and E_d^0 are the atomic energy levels corresponding to the reference free-atom state with N_s^0 and N_d^0 s and d valence electrons respectively and $\Delta N = N_d - N_d^0$. In practice, the bond energy is evaluated under the constraint that the numbers of s and d electrons on each site are kept fixed and equal to their reference values, respectively, through the adjustment of the atomic energy levels. It has been shown to be valid to first order [21].

2.2. *Bond energy in SCBLM*

The bond energy may be broken down in terms of contributions from individual pairs of bonds [20, 22] by writing equation (3) as

$$U_{\text{bond}} = \tfrac{1}{2} \sum_{ij,i\neq j}{}' U_{\text{bond}}^{ij} \tag{5}$$

where

$$U_{\text{bond}}^{ij} = 2 \sum_{\alpha\beta} H_{i\alpha,j\beta}\theta_{j\beta,i\alpha} \tag{6}$$

where the prefactor 2 accounts for spin degeneracy, H is the tight-binding matrix linking the orbitals on sites i and j together, and θ is the corresponding bond-order matrix whose elements are defined at energy E as [23]:

$$\theta_{j\beta,i\alpha}(E) = (2/\pi)\,\text{Im}\langle j\beta|(E + i0 - H)^{-1}|i\alpha\rangle. \tag{7}$$

We note here that, for a self-adjoint representation of H (that is, the tight-binding Hamiltonian), we can obtain

$$\mathrm{Im}\langle j\beta|(E+\mathrm{i}0-H)^{-1}|i\alpha\rangle = \tfrac{1}{2}\mathrm{Im}[\langle\phi_+|(E+\mathrm{i}0-H)^{-1}|\phi_+\rangle - \langle\phi_-|(E+\mathrm{i}0-H)^{-1}|\phi_-\rangle] \tag{8}$$

where

$$\phi_\pm = (1/\sqrt{2})(\phi_{j\beta} \pm \phi_{i\alpha}). \tag{9}$$

Equation (8) allows us to find again the definition of bond order given by Pettifor, by using the bonding G_+ and antibonding G_- Green functions [7,8]. Here, from equations (3), (5), (6) and (7), we write the bond order in terms of the imaginary part of the off-diagonal Green functions:

$$\theta_{j\beta,i\alpha} = \int^{E_F} \theta_{j\beta,i\alpha}(E)\,\mathrm{d}E = -\frac{2}{\pi}\int^{E_F} \mathrm{Im}\, G_{ij}^{\alpha\beta}(E)\,\mathrm{d}E. \tag{10}$$

In disordered systems such as liquids, instead of the LDOS $n_{i\alpha}(E)$ or the Green function $G_{ij}^{\alpha\beta}(E)$, we are interested only in configuration-averaged values. In order to calculate these quantities, we have used the SCBLM. One assumes that the mean local environment is isotropic, and then there is spherical point symmetry for the CBLM mean-field model [24]. This method is efficient to study s–d hybridization effects in disordered systems; in particular, one can use it to explain the positive Hall coefficient in some transition-metal disordered systems [25]. The question of the validity of the Bethe lattice approximation for hybridization is of course important, and Mayou *et al* [9] have shown that the geometrical local environment does not play a major role in the electronic structure of a liquid, provided that the average coordination number is sufficiently high ($\bar{Z} \geqslant 10$). In order to obtain the bond order in the SCBLM formalism we first recall the matrix expression of the Green function of an atom in CBLM [26]:

$$\mathbf{G}_I^{\mathrm{CBLM}}(z) = \left(z\mathbf{1} - \mathbf{E}_I - Z\sum_J p_{IJ}\mathbf{t}_{IJ}\mathbf{S}_{JI}(z)\right)^{-1} \tag{11}$$

where $I(i)$ denotes the species (A or B) at site i, p_{IJ} are the pair probabilities and $\mathbf{t}_{IJ}$ and $\mathbf{S}_{IJ}$ are the matrix of hopping energies and the so-called transfer matrix respectively. In the spherical approximation made by SCBLM, we obtain simple scalar equations for the Green function in the subspaces $\alpha(i)$ of atom i as [9]

$$G_{\alpha(i)}(z) = \left(z - E_{\alpha(i)} - Z\sum_{\beta(j)} \sigma^2_{\alpha(i),\beta(j)} G'_{\beta(j)}(z)\right)^{-1} \tag{12}$$

where one defines

$$\sigma^2_{\alpha(i),\beta(j)} = Z p_{IJ} n_\beta T^2_{\alpha(i),\beta(j)} \tag{13}$$

with n_β the degeneracy of subspace β and $T^2_{\alpha(i),\beta(j)}$ the mean square of the matrix element between a state of subspace α of atom i and a state of subspace β of atom j (see equation (10) in [9]). Finally $G'_{\beta(j)}(z)$ can be defined by

$$G'_{\beta(j)}(z) = \left(z - E_{\beta(j)} - \sum_{\gamma(k)} (\sigma'_{\beta(j),\gamma(k)})^2 G_{\gamma(k)}(z)\right)^{-1} \tag{14}$$

with

$$(\sigma'_{\beta(j),\gamma(k)})^2 = [(Z-1)/Z](\sigma_{\beta(j),\gamma(k)})^2.$$

By comparing (11) with (12) and (13) it follows that

$$t_{\alpha(i),\beta(j)} S_{\beta(j),\alpha(i)}(z) = n_\beta T^2_{\alpha(i),\beta(j)} G'_{\beta(j)}(z). \tag{15}$$

On the other hand, the transfer matrix S is related to the off-diagonal Green function by

$$G_{\beta(j),\alpha(i)}(z) = \sum_\alpha S_{\beta(j),\alpha(i)}(z) G_{\alpha(i),\alpha(i)}(z) = n_\alpha S_{\beta(j),\alpha(i)}(z) G_{\alpha(i)}(z). \tag{16}$$

By using (7), (15) and (16), we obtain the bond potential from (6) as

$$\begin{aligned} U^{ij}_{\text{bond}} &= -\frac{2}{\pi} \sum_{\alpha\beta} t_{\alpha(i),\beta(j)} \operatorname{Im} \int^{E_F} [n_\alpha S_{\beta(j),\alpha(i)}(E) G_{\alpha(i)}(E)] \, \mathrm{d}E \\ &= -\frac{2}{\pi} \sum_{\alpha\beta} \operatorname{Im} \int^{E_F} [n_\alpha n_\beta T^2_{\alpha(i),\beta(j)} G_{\alpha(i)}(E) G'_{\beta(j)}(E)] \, \mathrm{d}E \\ &= \sum_{\alpha\beta} \Phi^{\text{bond}}_{\alpha(i),\beta(j)}. \end{aligned} \tag{17}$$

From equation (17) it is clear that, in our formalism, the bond potential interaction can be expressed directly from the local Green functions treated in the mean isotropic environment. We note that the expression (17) is also valid in the more general case of a binary alloy. There is no difficulty to show that $\theta_{\alpha(i),\beta(j)} \sim Z^{-1/2}$ as a property of the Bethe lattice system [22]. For a pure metal, the bond order on the Bethe lattice can be obtained from (17) by putting $p_{IJ} = 1$ in equations (11) and (13). In the last case, we have

$$\Phi^{\text{bond}}_{\alpha(i),\beta(j)} = \Phi^{\text{bond}}_{\beta(i),\alpha(j)} \tag{18}$$

in the limit of $Z \to \infty$. The advantage of equation (17) is that it allows us to estimate the different orbital contributions in the bond energy, in particular, to treat the effect of hybridization explicitly. Assuming that the bond order $\theta_{j(\beta),i(\alpha)}$ in equation (10) is a slowly varying function of the bond length, we obtain

$$\Phi^{\text{bond}}_{\alpha(i),\beta(j)} = t_{\alpha(i),\beta(j)} \theta_{\beta\alpha} \tag{19}$$

with the distance dependence of the hopping integral $t_{\alpha(i),\beta(j)}$. Here the average hopping integrals are evaluated according to Harrison's power-law dependence [27]:

$$(ll'm) = \eta_{ll'm}h^2/mr^2 \tag{20a}$$

for s and p electrons and

$$(ll'm) = \eta_{ll'm}h^2/mr^{l+l'+1} \tag{20b}$$

for other electrons.

2.3. Pair potential and universality of the binding energy

To determine the repulsive part of the total energy, we assume repulsive pairwise interactions proportional to r^{-p} that are capable of reproducing the behaviour of the bulk modulus across the 3d transition-metal series as has been fitted by WH to obtain the values of pseudopotential parameter r_c (the empty core radius). Another fitting may be made by requiring that at $T = 0$ K the energy is minimum at the observed volume of the metal, but as has been emphasized by Regnaut [5] in the WH model, it is more difficult in this case to obtain a shallower potential well shifted towards a large value of interatomic distance. As the repulsive energy of the system is constructed from s and d-electron contributions, we have

$$\Phi_{rep}(r_{ij}) = \Phi^s_{rep}(r_{ij}) + \Phi^d_{rep}(r_{ij}) \tag{21}$$

with

$$\Phi^s_{rep} = C_s/r^4_{ij} \tag{22a}$$

and

$$\Phi^d_{rep} = C_d/r^{15}_{ij} \tag{22b}$$

where C_s and C_d are two unknown structure-dependent parameters (see appendix). The justification of the distance dependence used in equations (22*a*) and (22*b*) and their relations with the expressions (20*a*) and (20*b*) are given below. Then, in addition to the experimental bulk modulus, we use the experimental equilibrium volume of the 3d metals to obtain the second parameter [28]. We have also verified that these parameters are not strongly modified by a decrease of 10% of the crystal bulk modulus. The experimental values of the atomic volume Ω_0, bulk modulus B and the corresponding calculated parameters of the repulsive interactions are also presented in table 1. In figure 1, we present pair potentials calculated with our model for the 3d liquid transition metals. These total effective interatomic potentials can be decomposed into contributions from s and d electrons, and we use a coordination number of $Z = 12$ corresponding to the close-packed crystalline and liquid metals. As shown in this figure, the variation of s and d hybridized band potential contributions across the 3d series implies that the full potential has a larger d-like attractive well at the middle and at the beginning of the series. The pair potential of the late 3d

Table 1. Input parameters for the calculations of the interatomic forces: liquid temperature T, atomic volume Ω_0, bulk modulus B. The corresponding calculated constants C_s, C_d are presented in the last two columns.

Element	T_{fusion} (°C)	Ω_0 (Å^3)	B (10^{11} N m^{-2})	C_s (eV)	C_d (eV)
Ti	1700	19.15	1.051	1.0574	0.1153
V	1900	15.77	1.619	1.5751	0.1498
Cr	1900	13.76	1.901	2.0416	0.1558
Mn	1260	15.27	0.596	1.8744	0.0449
Fe	1550	13.22	1.683	1.4389	0.1208
Co	1550	12.70	1.914	0.7790	0.1306
Ni	1500	12.61	1.860	0.7003	0.1158
Cu	1150	13.28	1.370	0.2865	0.0861

metals (Ni, Cu) is expected to be dominated by the s-like contribution. This behaviour emphasizes the important role of the s–d hybridization effect in studying the atomic structure of transition-metal liquids.

The last point upon which we would like to comment in this section concerns the scaling problem of the binding energy when the repulsive and attractive pair interactions are parametrized by a power law as $(r_0/r)^p$ and $(r_0/r)^q$. It is well known that by using the pair interactions parametrized as simple exponentials one can derive binding energy–distance universal relations valid for transition metals [22, 29, 30]. In particular, Abel [22] has found for the one-band case, when the bulk band energy per atom can be written as

$$E_b(r) = Z[Aa\exp(-pr) - Bb\exp(-qr)] \tag{23}$$

that the structure dependence of the scaling cohesive energy $D_e^* = -E_B(y, s)$ at the scaling equilibrium interatomic distance $y = y_e$ (see appendix) is given by the following expression:

$$D_e^* = Z(a/b)^{s/(s-1)}. \tag{24}$$

Here $s = p/q$ and a and b are structure-dependent parameters characterizing the net electron density and the bond order, respectively; A and B are positive quantities characteristic for a given atomic species. The ratio s is constant along transition-metal series with values between 2 and 5. It is not difficult to show (see appendix) that the relation (24) is valid not only for the exponential model but also for the power-law expression:

$$E_b(r) = Z[Aa(1/r^p) - Bb(1/r^q)] \tag{25}$$

chosen in this paper. It allows us to justify the values of $s = 2$ and 3 for s- and d-band contributions, respectively, used in our calculations.

On the other hand, the transferability of the TB parameters can be improved by modifying their functional forms as suggested by Goodwin [31]. Following these authors, we have also chosen to introduce a smoothed step function to reduce the range of the atomic interactions; this effect is noticeable for the late 3d metals in which the s-like contribution becomes important. The two scaling smoothed step

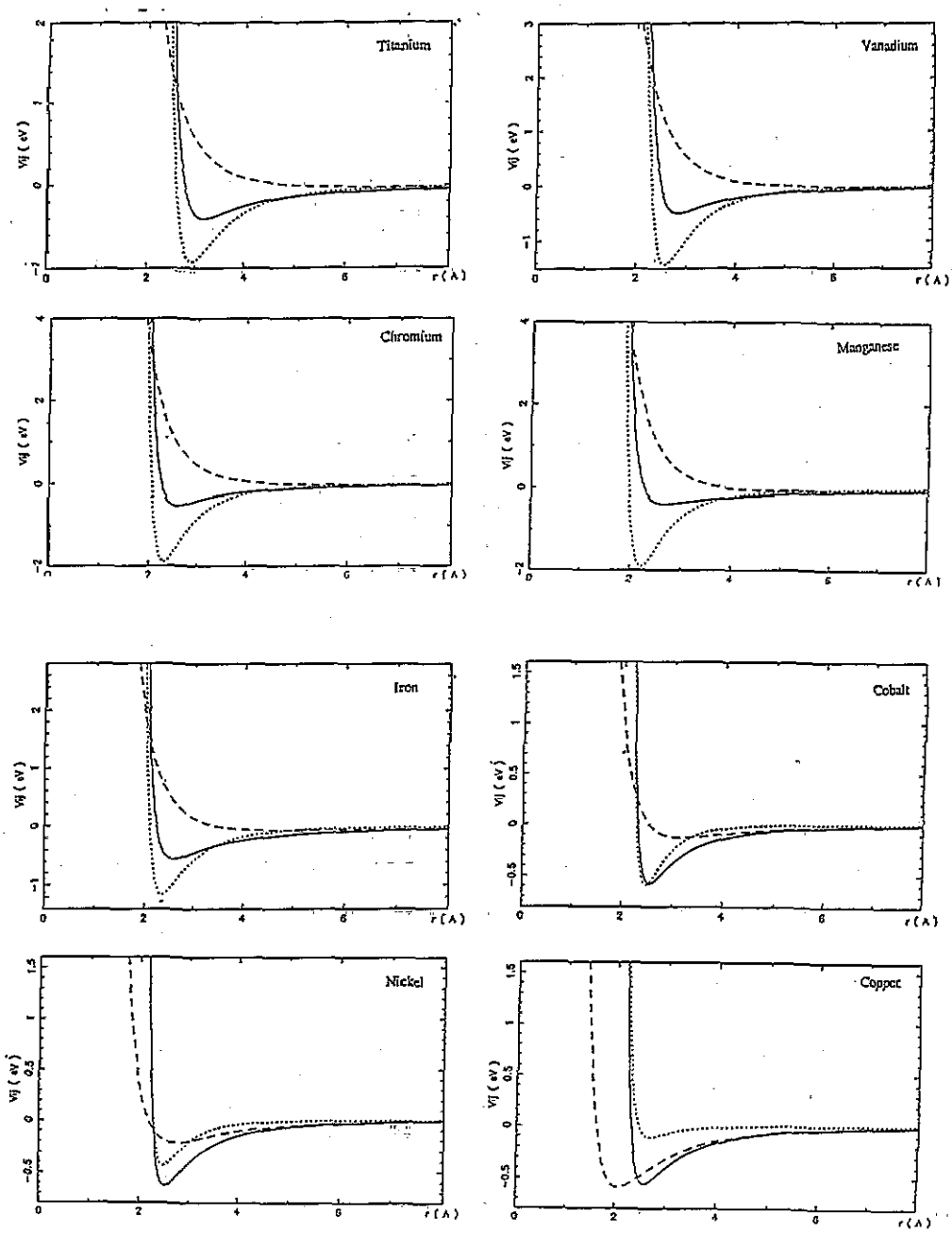

Figure 1. Interatomic potential obtained from our calculations for the liquid 3d transition metals. The full curve corresponds to the total potential, the broken curve to the s-hybridized contribution and the dotted curve to the d-hybridized contribution.

functions have been chosen in such a way that the step is positioned between the first and the second nearest neighbours in the FCC lattice and that the interactions become zero at $L/2$, where L is the linear dimension of the molecular dynamic cell.

3. The liquid structure of the 3d transition metals

3.1. Molecular dynamics simulations

We have used our interactomic interactions in a standard microcanonical NVE molecular dynamics (MD) investigation of liquid structure of the 3d transition metals. Our molecular dynamics routines are based on integrating the equations of motion in a velocity form of the Verlet algorithms [32]. A 1332-particle cluster with periodic boundary conditions is used and the lattice parameter of the molecular dynamics cell is expanded to give the required liquid density [28]. The time increment h in our simulations is chosen to be approximately 10^{-15} s. The liquid is then 'heated' by raising initial temperature and subsequently scaling it down to the required value. Typical simulations run up to $(3–4) \times 10^4$ steps.

3.2. Results

The pair correlation functions $g(r)$ are calculated for 3d transition metals after averaging over about 250–300 independent configurations taken at intervals at 100 time steps. In order to verify the shouldered effect of the s–d hybridized potential, we present in figure 2 the results of $g(r)$ calculated for both cases: with the full potential and with only the d part for Ti, Fe and Ni. It is clear from this figure that the very deep potential well predicted in the second case leads to a noticeable change in the theoretical determination of the first peak magnitude of $g(r)$ for a transition metal with less than half-filled (Ti) and with half-filled (Fe) d bands. This remark is in agreement with Regnaut's discussion on the validity of WH potentials [5]. The static structure factors $S(q)$ for all the 3d elements are given in figure 3. Note that our molecular dynamics simulation achieves a good fit to the diffraction data [33] including the lightest 3d metal Ti and V [34]. By remembering that there are only two experimental data to parametrize the interatomic interactions constructed in our s–d hybridization formalism, we think that they can serve as a basis for reliable simulations of liquid transition metals.

4. Electronic structure and total energy of the 3d liquid transition metals

4.1. Electronic density of states

In order to test the validity of our interatomic interactions, we have also calculated the electronic density of states of the molten 3d transition metals, from the atomic coordinates obtained by molecular dynamics simulations. Using the same tight-binding Hamiltonian, the recursion method has been used and we have stopped the recursion after about 12 levels for s and d orbitals. The site-averaged DOS was calculated for a sample of 10 atoms randomly chosen among the innermost atoms. The electronic densities of states of the 3d liquid transition metals are shown in figure 4. Although the global behaviour of the total DOS can be dominated by the d-band contribution, the s–d hybridization effect can lead to a decrease in the s DOS inside the d band as has been shown by Mayou *et al* [9]. Except for the cases of Ti and V, where band narrowing is expected in comparison with the crystalline case because of the large volume expansion in the liquid state, we have found that the bandwidth is the same in the molten and crystalline states. Figure 4 displays the characteristic bonding–antibonding splitting in the d band as has been obtained from the supercell linear

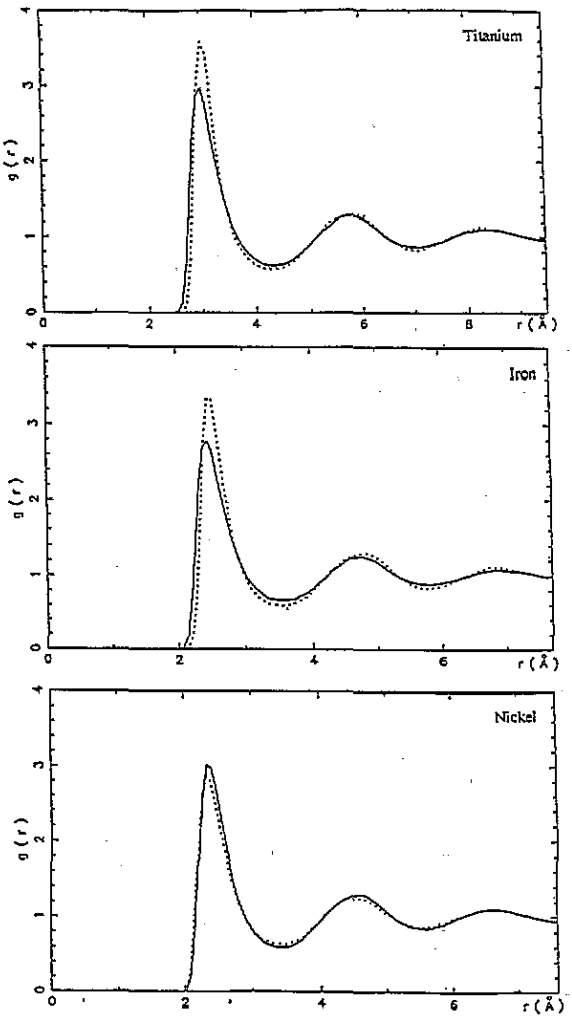

Figure 2. Pair correlation function $g(r)$ obtained from MD simulations for three representative liquid transition metals of the 3d series: Ti, Fe and Ni. Full curves are calculated from total hybridized s–d potential and dotted curves from d potential without hybridization.

muffin-tin orbital (LMTO) approach of Jank *et al* [35]. In table 2 our calculated DOS at the Fermi level for the 3d liquid elements are compared with the data of Jank *et al* and with those estimated from the magnetic susceptibilities [36].

4.2. Hybridization bond energy

The bond energy can be calculated in two different ways: it can be obtained either from the average DOS calculated by a recursion method or from the attractive part of the interatomic interactions; in this case, we use an average interatomic distance and an average coordination number deduced from the position and the area of the first peak of the pair correlation function respectively. The results of both estimations are compared in table 3 and show good agreement between these two methods.

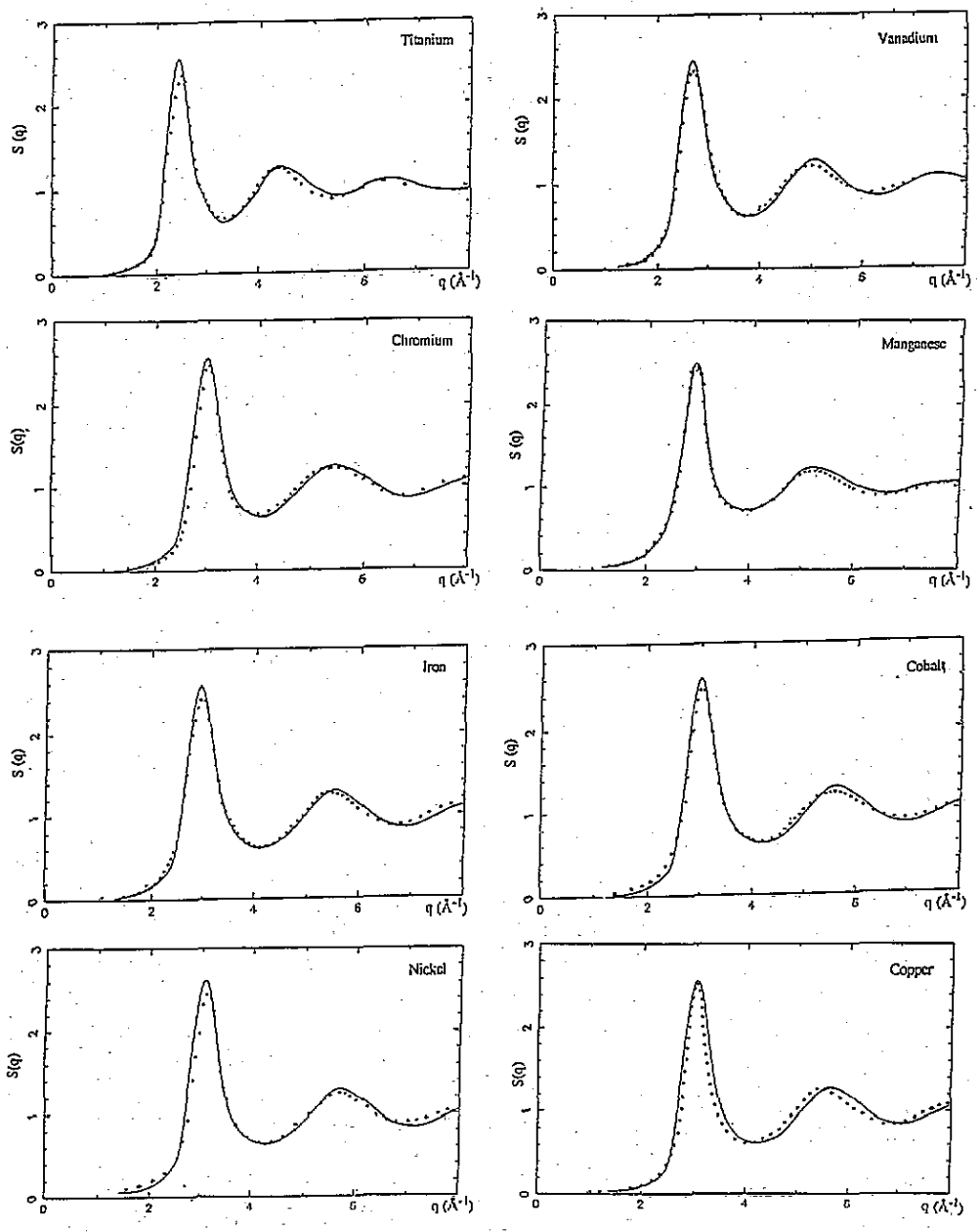

Figure 3. Static structure factor $S(q)$ for liquid 3d transition metals from Ti to Cu. Full curves: MD simulation. Dotted curves: experiment [33].

Another interesting aspect is the role played by s–d hybridization in the bonding energy of the transition-metal systems. This problem has been analysed in detail with the renormalized atom approximation for the 3d and 4d series [16]. However, in this work, the s–d hybridization terms have been estimated by a semiquantitative partitioning of their contributions across the series. As has been shown in section 2 the total bonding energy in our approach may be written as

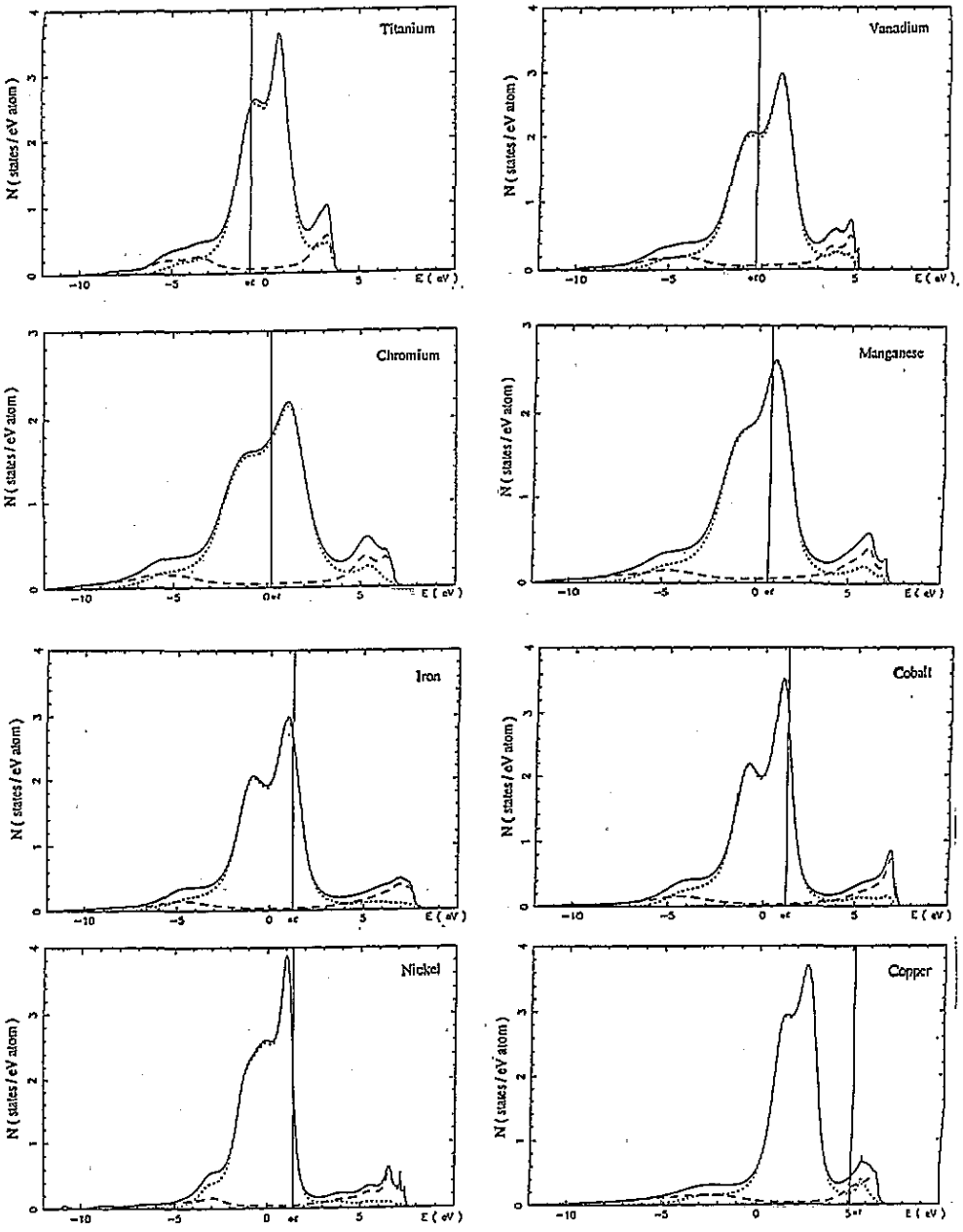

Figure 4. *Calculated electronic density of states for the liquid 3d transition metals. Full* curves correspond to the total DOS, broken curves to s partial DOS and dotted curves to d partial DOS. The Fermi energy is marked with a vertical line labelled ef.

$$E_{\text{total}}^{\text{bond}} = E_{\text{s-s}}^{\text{bond}} + 2E_{\text{s-d}}^{\text{bond}} + E_{\text{d-d}}^{\text{bond}} \tag{26}$$

with

$$E_{\text{s-d}}^{\text{bond}} = E_{\text{d-s}}^{\text{bond}}.$$

Table 2. Comparison of our calculated density of states at the Fermi level with the supercell approach [35] and with experimental ones for liquid Mn, Fe, Co and Ni [36].

	$n(E_F)$ (states/eV atom)		
Element	Calculated from this paper	Calculated from [35]	Experiment [36]
Mn	2.50	2.34	2.40
Fe	2.63	2.59	2.60
Co	3.02	2.99	2.95
Ni	1.92	2.10	2.10

Table 3. The calculated total bond energy obtained from the calculated DOS and from the SCBLM self-consistent calculations. The fourth column shows the ratio of the s–d hybridized contribution to the total bond energy for the liquid 3d transition metal.

Element	E_{total}^{bond} (from calculated DOS) (eV)	E_{total}^{bond} (from SCBLM self-consistent calculations) (eV)	$\frac{2E_{s-d}^{bond}}{E_{total}^{bond}}$
Ti	−10.22	−10.17	0.52
V	−15.06	−14.98	0.49
Cr	−17.89	−17.97	0.47
Mn	−14.94	−14.96	0.49
Fe	−13.14	−13.22	0.52
Co	−10.73	−10.67	0.46
Ni	− 9.76	− 9.70	0.63
Cu	− 5.38	− 5.46	0.42

Table 4. Heat of fusion for the liquid 3d transition metals. Theory: calculated in the CBLM approach. Experiment: from [40].

Element	$E_{fusion}^{calculated}$ (kJ mol^{-1})	$E_{fusion}^{experiment}$ (kJ mol^{-1})
Ti	16.75	15.59
V	17.08	15.58
Cr	14.22	14.63
Mn	14.85	14.63
Fe	14.70	15.05
Co	16.23	16.51
Ni	17.85	17.22
Cu	13.69	12.96

The ratio $2E_{s-d}^{bond}/E_{total}^{bond}$ is also presented in table 3 to emphasize the important percentage of s–d hybridization in bonding energies. It gives about 50% for all elements of the 3d series and it is about 60% for Ni liquid. For the last case, it is clear from figure 1 that, at the equilibrium position of the melt state, the s-like contribution of the pair potential becomes negative due to the hybridization effects.

4.3. The heat of fusion

By definition, the heat of fusion may be estimated by comparing the cohesive energies

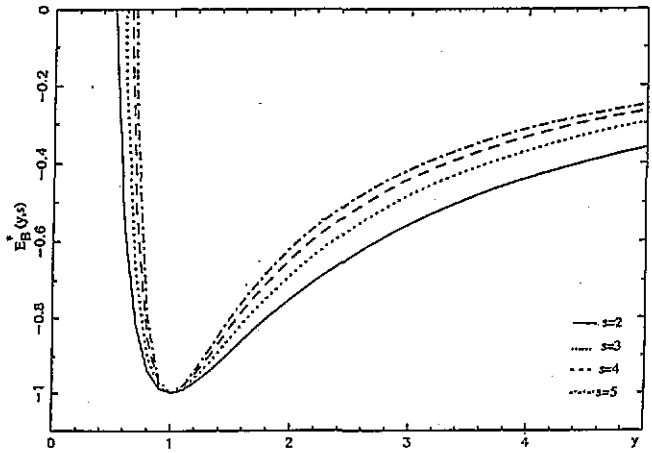

Figure 5. Plot of the scaled bonding energy $E_B^*(y, s)$ versus y for different values of s.

in the solid and liquid states at the melting temperature [39]:

$$L_f = E_{coh}^{solid} - E_{coh}^{liquid}. \tag{27}$$

We have calculated the values of E_{coh}^{liquid} from equation (1) with the help of equations (2), (3) and (26) and those of E_{coh}^{solid} on the same basis, i.e. using CBLM formalism coupled with the same tight-binding Hamiltonian. The results of calculations are presented in table 4; they show a good agreement with the experimental values [40].

5. Discussions and conclusions

We have constructed interatomic potentials based on the SCBLM formalism that takes into account the important s–d hybridization effect for the transition-metal systems. The expressions of the potentials are general and they can be applied to study liquid or amorphous alloys. The short-range order in these systems may be incorporated in a self-consistent manner and the results will be published elsewhere. In this paper we have used this formalism to study the atomic and electronic structure of the liquid 3d transition metals. We have found that the s–d hybridization effects improves the description of the liquid structure not only for the late 3d elements but also for the half-filled and less than half-filled ones. These correct trends for the 3d liquid structure have been confirmed by: (i) the good agreement of the static structure factors obtained from our molecular dynamics simulations with the experimental ones; (ii) the TB DOS, which are similar to those calculated from *ab initio* calculations; and (iii) the theoretical results of the heat of fusion, which are in agreement with the experimental ones. These results are very promising and may be explained by the fact that we have obtained a decisive improvement in the treatment of s electrons in comparison with the WH model. In this model, s–d hybridization is only treated by changing the relative occupancies of the s and d bands, so that the most important effect of band mixing between s and d bands is neglected. Our formalism is based on Pettifor's description of the bonding energy, but

the contributions of multi-ion terms are not taken into account in our study, owing to the Bethe lattice self-consistent approximation. However, as has been explained previously, it allows us to incorporate the hybridization effects in a simple way and therefore the bond energy can be associated explicitly through the fourth moment of the local density of states. Therefore, these effective pair potentials are naturally better than those obtained from the embedded atom models, which are valid only within the second moment approximation.

Acknowledgments

We are grateful to Professor C Colinet (LTPCM) and Dr D Mayou (CNRS) for helpful discussions. Fruitful conversations with Professor G J Morgan (University of Leeds) on the tight-binding bond approach are also acknowledged. One of us (D Nguyen Manh) would like to thank CNRS for financial support and LTPCM for its hospitality.

Appendix

When the repulsive and attractive pair interactions are parametrized as a power law, the bonding energy for a given structure in the one-band case is

$$E_B(r) = Z\left[Aa\frac{1}{r^p} - Bb\frac{1}{r^q}\right]. \tag{A1}$$

The equilibrium interatomic separation r_e is determined from $[dE_B(r)/dr]|_{r=r_e} = 0$, which gives

$$r_e = \left(\frac{Aap}{Bbq}\right)^{1/(p-q)} \tag{A2}$$

and

$$D_e = -E_B(r_e) = ZAa(s-1)(1/r_e^p) = ZBb[s/(s-1)](1/r_e^q) \tag{A3}$$

where D_e is the cohesive energy and

$$s = p/q. \tag{A4}$$

From (A1)–(A3) the scaling procedure is

$$E_B^*(r) = \frac{E_B(r)}{D_e} = \frac{1}{s-1}\left[\left(\frac{r_e}{r}\right)^p - s\left(\frac{r_e}{r}\right)^p\right]. \tag{A5}$$

If one defines

$$l^2 = \frac{D_e}{[d^2E_B(r)/dr^2]|_{r=r_e}} \tag{A6}$$

then it is not difficult to find

$$l = r_e/(pq)^{1/2}. \tag{A7}$$

Substituting (A7) into (A5) gives

$$E_B^*(y,s) = \frac{1}{s-1}\left[\left(\frac{1}{y}\right)^s - s\left(\frac{1}{y}\right)\right] \tag{A8}$$

with

$$y^{-1} = (r_e/r)^q = [(1/r)(pq)^{1/2}]^q. \tag{A9}$$

In figure 5 we show the dependence of the scaled bonding energy (A8) as a function of y for different values of $s = p/q$.

In order to analyse the structure dependence of D_e we introduce a scaling procedure that retains the structure variables a and b. One defines

$$E_B^*(y,s) = \frac{E_B(r)}{aD_{e2}} \tag{A10}$$

with

$$D_{e2} = A(s-1)\frac{1}{r_{e2}^p} = B\frac{(s-1)}{s}\frac{1}{r_{e2}^q} \tag{A11}$$

with

$$r_{e2} = (sA/B)^{1/(p-q)} \tag{A12}$$

so

$$r_e = (a/b)^{1/(p-q)} r_{e2}. \tag{A13}$$

This scaling gives

$$E_B^*(y,s) = \frac{Z}{s-1}\left[a\left(\frac{1}{y}\right)^s - bs\left(\frac{1}{y}\right)\right] \tag{A14}$$

with

$$y^{-1} = (r_{e2}/r)^q. \tag{A15}$$

Therefore from

$$\left[\frac{\mathrm{d}E_B^*(y,s)}{\mathrm{d}y}\right]\Bigg|_{y=y_e} = 0$$

we have

$$y_e = (b/a)^{1/(s-1)} \tag{A16}$$

and

$$D_e^* = -E_B^*(y_e, s)$$

or

$$D_e^* = Z(b/a)^{s/(s-1)}. \tag{A17}$$

Equation (A17) has exactly the same expression as those obtained from exponential parametrization (see equation (28) of [22]). For the FCC lattice ($Z = 12$), the recursion method gives b(FCC) = 0.206 with $a = 1$; so using equation (A17) one obtains $s = 2.7$.

References

[1] Wills J M and Harrison W A 1983 *Phys. Rev.* B **28** 4363
[2] Bretonnet J L and Derouiche A 1991 *Phys. Rev.* B **43** 8924
[3] Hausleitner C and Hafner J 1988 *J. Phys. F: Met. Phys.* **18** 1025
[4] Bretonnet J L, Bhuiyan G M and Silbert M 1992 *J. Phys.: Condens. Matter* **4** 5359
[5] Regnaut C 1989 *Phys. Rev.* B **76** 179
[6] Moriarty J A 1988 *Phys. Rev.* B **38** 3199
[7] Pettifor D G 1990 *Many-Atom Interactions in Solids* ed R M Nieminen, M J Puska and M J Manninen (Berlin: Springer) p 64
[8] Pettifor D G and Aoki M 1991 *Phil. Trans. R. Soc.* A **334** 439
[9] Mayou D, Nguyen Manh D, Pasturel A and Cyrot Lackmann F 1986 *Phys. Rev.* B **33** 3384
[10] Nguyen Manh D, Mayou D, Pasturel A and Cyrot Lackmann F 1985 *J. Phys. F: Met. Phys.* **15** 1911
Nguyen Manh D, Mayou D, Cyrot Lackmann F and Pasturel A 1987 *J. Phys. F: Met. Phys.* **17** 1039
Nguyen Manh D, Dinh Hoai G, Pasturel A and Colinet C 1991 *Physica* B **173** 293
[11] Pasturel A, Hafner J and Mayou D 1988 *Z. Phys. Chem.* NF **157** 53
[12] Robbins M O 1983 *PhD Thesis* University of California, Berkeley, p 104
[13] Finnis M W and Sinclair J E 1984 *Phil. Mag.* A **50** 45
[14] Daw M S and Baskes M I 1984 *Phys. Rev.* B **29** 6443
[15] Hausleitner C and Hafner J 1992 *Phys. Rev.* B **45** 115
[16] Gelatt C D Jr, Ehrenreich H and Watson R E 1977 *Phys. Rev.* B **15** 1663
[17] Harris J 1985 *Phys. Rev.* B **31** 1770
[18] Anderson P W 1968 *Phys. Rev. Lett.* **21** 13
[19] Andersen O K and Jepsen O 1984 *Phys. Rev. Lett.* **53** 2571
[20] Sutton A P, Finnis M W, Pettifor D G and Ohta Y 1988 *J. Phys. C: Solid State Phys.* **21** 35
[21] Cressoni J C and Pettifor D G 1991 *J. Phys.: Condens. Matter* **3** 495
[22] Abell G C 1985 *Phys. Rev.* B **31** 6184
[23] Kelly M J 1980 *Solid State Physics* vol 35, ed H Ehrenreich, F Seitz and D Turnbull (New York: Academic) p 302
[24] Robbins M O and Falicov L M 1984 *Phys. Rev.* B **29** 1333
[25] Nguyen Manh D, Mayou D, Morgan G J and Pasturel A 1987 *J. Phys. F: Met. Phys.* **17** 999
[26] Nguyen Manh D 1986 *PhD Thesis* University of Grenoble
[27] Harrison W A 1980 *Electronic Structure and the Properties of Solids* (San Francisco: Freeman)
[28] Waseda J Y 1977 *Liquid Metals (Inst. Phys. Conf. Ser. 30)* p 230
[29] Rose H, Ferrante J and Smith J R 1983 *Phys. Rev.* B **28** 1835
[30] Spanjaard D and Dejonquères M C 1984 *Phys. Rev.* B **30** 4822

[31] Goodwin L, Skinner A J and Pettifor D G 1989 *Europhys. Lett.* 9 701
[32] Heermann D W and Burkitt A N 1991 *Parallel Algorithms in Computational Science* (Berlin: Springer)
[33] Waseda Y 1981 *The Structure of Non-Crystalline Materials–Liquids and Amorphous Solids* (New York: McGraw-Hill)
[34] Hausleitner C, Kahl G and Hafner J 1991 *J. Phys.: Condens. Matter* 3 1589
[35] Jank W, Hausleitner C and Hafner J 1991 *J. Phys.: Condens. Matter* 3 4477
[36] Buch G and Guntherodt H J 1974 *Solid State Physics* vol 29, ed H Ehrenreich, F Seitz and D Turnbull (New York: Academic) p 235
[37] Ducastelle F 1972 *Dr Sci Thesis* Université de Paris-Sud, Orsay
[38] Paxton A T, Methfessel M and Polatoglou H M 1990 *Phys. Rev.* B 41 8127
[39] Cyrot Lackmann F 1968 *Dr Sci Thesis* Université de Paris-Sud, Orsay
[40] Gschneider K A 1964 *Solid State Physics* vol 16, ed H Ehrenreich, F Seitz and D Turnbull (New York: Academic) p 275